Vol 17 No 1, January 2008
1674-1056/2008/17(01)/0158-06

Chinese Physics B

© 2008 Chin. Phys. Soc.
and IOP Publishing Ltd

Line intensities of the asymptotic asymmetric-top radical HO_2 at high temperatures*

Song Xiao-Shu(宋晓书)[a)b)], Cheng Xin-Lu(程新路)[b)], Yang Xiang-Dong(杨向东)[b)†], Linghu Rong-Feng(令狐荣锋)[a)], and Lv Bing(吕 兵)[a)]

[a)] *School of Physics and Chemistry, Guizhou Normal University, Guiyang* 550001, *China*
[b)] *Institute of Atomic and Molecular Physics, Sichuan University, Chengdu* 610065, *China*

(Received 11 February 2007; revised manuscript received 26 May 2007)

The total internal partition sums were calculated in the product approximation at temperatures up to 5000 K for the asymptotic asymmetric-top HO_2 molecule. The calculations of the rotational partition function and the vibrational partition function were carried out with the rigid-top model and in the harmonic oscillator approximation, respectively. Our values of the total internal partition sums are consistent with the data of HITRAN database with −0.14% at 296 K. Using the calculated partition functions, we have calculated the line intensities of ν_2 band of HO_2 at several high temperatures. The results showed that the calculated line intensities are in very good agreement with those of HITRAN database at temperatures up to 3000 K, which provides a strong support for the calculations of partition functions and line intensities at high temperatures. Then we have extended the calculation to higher temperatures. The simulated spectra of ν_2 band of the asymptotic asymmetric-top HO_2 molecule at 4000 and 5000 K are also obtained.

Keywords: asymptotic asymmetric-top molecule, line intensities, partition functions, high temperature

PACC: 3310, 3320E

1. Introduction

Molecular spectrum is one of the most important methods for studying molecular structure and also is of importance in astrophysics. Using this technique we can not only detect the presence of various molecules on fixed stars, planets, and comets, in the upper atmosphere, and in interstellar space based on their spectra, but also draw definite conclusions concerning the physical conditions in these objects from a more detailed analysis.[1] In recent years, with the development of astrophysics and atmospheric sciences, molecular spectra have been widely used in remote sensing measurements, the identification of objective characteristics, environmental pollution and atmospheric radiation and transfers.[2,3] The hydroperoxyl, HO_2, as a prototypical light asymmetric-top free radical, is of importance in both atmospheric and combustion chemistry. It has now been thoroughly studied in its ground state with a variety of spectroscopic techniques.[4−8] However, all these studies were made at normal temperature. Up to now, a plenty of spectral measurements in experiment and theoretical calculations have still focused on normal and mid-high temperatures.[9−16] In HITRAN database, we can only obtain the line intensities at temperatures up to 3000 K by extrapolating method.[17] With the rapid development of aeronautics, the study of molecular spectrum at higher temperatures has been becoming very necessary. Recently, our work has focused on high-temperature molecular spectrum. We produced the line intensities of vibration–rotation transition at temperatures up to 5000 K on the basis of our calculated partition function. In our previous papers, we reported the high-temperature spectra of linear molecules.[18−20] Here, we concentrate on the calculation of the transition line intensities of asymptotic asymmetric-top molecule HO_2 at high temperatures. The line intensities of the ν_2 band of HO_2 are obtained by directly calculating partition function at normal and several high temperatures. Comparing with the values obtained from HITRAN database, the results show that the agreement between the calculated line intensities and those extrapolated from HITRAN database is fairly good for the ν_2 band of HO_2 at temperatures up to 3000 K, which provides a

*Project supported by the Major Program for Basic Research of National Security, China (Grant No 5134202-04), by the National Natural Science Foundation of China (Grant No 10574096), and the Natural Science Foundation of the Bureau of Education of Guizhou Province, China (Grant No 2006204).

†E-mail: buttly2006@126.com

strong support for the calculations of partition function and line intensities at high temperatures. So we calculate the total internal partition sums (TIPS) and line intensities of HO_2 at higher temperatures of 4000 and 5000 K. Meanwhile, we also present the simulated spectra of ν_2 band of HO_2 at the same high temperatures. The results are of significance for the studying of molecular spectra at high temperatures.

2. Details of the calculation

2.1. Partition functions

The total internal partition sums were calculated in the product approximation[21]

$$Q(T) = Q_{\rm vib} \times Q_{\rm rot}. \tag{1}$$

The vibrational partition functions $Q_{\rm vib}$ were calculated using the harmonic oscillator approximation[22]

$$Q_{\rm vib}(T) = \prod_{\nu_i} \frac{1}{1-\exp\left(hc\nu_{\rm i}/k_{\rm B}T\right)}, \tag{2}$$

where h is the Planck's constant, c is the velocity of light in vacuum, ν_i is the fundamental vibrational frequency, $k_{\rm B}$ is the Boltzmann constant, T is the temperature. The high-temperature asymptotic expansion of the rotational partition function of a rigid asymmetric-top molecule can be written in the form[23]

$$Q = \bar{g}Q' + \sum_{\xi=a,b,c} g_\xi Q'_\xi, \tag{3}$$

where $\bar{g}$ is the mean nuclear statistical weight given by

$$\bar{g} = \frac{1}{\sigma}\prod(2I+1). \tag{4}$$

Here $\prod(2I+1)$ is the total number of nuclear spin functions and σ is the symmetry number, the order of the rotational subgroup of the molecular point group, and g_ξ is a nuclear statistical weight factor associated with the principal axis ξ. If this axis is not a proper axis of asymmetry of the molecular point group, the coefficient vanishes. If the a-axis is a twofold axis of symmetry, we have

$$g_a = \chi_{\rm ev}(C_{2a}) \prod_i^{a-{\rm axis}} (2I_i+1) \times \prod_j^{C_{2a-{\rm pairs}}} (-1)^{2I_j}(2I_j+1), \tag{5}$$

where the first factor is the character of the vibronic wavefunction under the symmetry operation C_{2a}, the I product is over all nuclei on the a-axis, and the j product has one factor for each pair of equivalent nuclei related by the C_{2a} operation. Similar formulae apply for g_b and g_c. The asymptotic expansion of Q' is expressed in the formulation of McDowell as

$$Q' = \left(\frac{\pi}{\alpha\beta\gamma}\right)^{1/2} {\rm e}^{f_1}(1+f'_2+f'_3+\cdots), \tag{6}$$

where

$$f_1 = \frac{1}{12}\left[2\sum\alpha - \sum\frac{\alpha\beta}{\gamma}\right], \tag{7}$$

$$f'_2 = \frac{1}{90}\sum\frac{\alpha\beta(\gamma-\alpha)(\gamma-\beta)}{\gamma^2}, \tag{8}$$

$$f'_3 = \frac{1}{2835}\sum\frac{(\gamma-\alpha)(\gamma-\beta)}{\gamma^3} \times\{(\alpha-\beta)^2\gamma^2 + 4(\alpha+\beta)\alpha\beta\gamma - 8\alpha^2\beta^2\}. \tag{9}$$

Here, α, β and γ are the dimensionless temperature-reduced rotational constants $hcA/k_{\rm B}T, hcB/k_{\rm B}T$ and $hcC/k_{\rm B}T$, and each sum is taken over the three cyclic permutations of (α, β, γ). For Q'_ξ, the principal asymptotic approximations are

$$Q'_{a0} = \left(\frac{\pi}{\alpha}\right)^{3/2}\exp(-\pi^2/4\alpha) \times \sec\left\{\frac{\pi\sqrt{[(\alpha-\beta)(\alpha-\gamma)]}}{2\alpha}\right\}, \tag{10}$$

$$Q'_{b0} = \left(\frac{\pi}{\beta}\right)^{3/2}\exp(-\pi^2/4\beta) \times \sec{\rm h}\left\{\frac{\pi\sqrt{[(\alpha-\beta)(\beta-\gamma)}}{2\beta}\right\}, \tag{11}$$

$$Q'_{c0} = \left(\frac{\pi}{\gamma}\right)^{3/2}\exp(-\pi^2/4\gamma) \times \sec\left\{\frac{\pi\sqrt{[(\alpha-\gamma)(\beta-\gamma)}}{2\gamma}\right\}. \tag{12}$$

For HO_2, the rotational constants A, B and C are taken from the work of Barnes *et al.*[24] The fundamental vibrational frequencies are obtained from Ref.[25]. The calculated values for $Q_{\rm vib}$, $Q_{\rm rot}$ and $Q(T)$ are 1.006, 4268.652, and 4294.272 at 296 K, respectively. The value of the total internal partition function $Q(T)$, 4294.272, is comparable to that of HITRAN database, 4300.4, with a deviation −0.14% at 296 K.

2.2. Line intensities

Line intensities were computed with the conventional formula[26]

$$S_{b\leftarrow a}(T) = \frac{8\pi^2 I_x}{3hc}\nu_{b\leftarrow a}\frac{g_a \exp(-hcE_a/k_BT)}{Q(T)} \times[1-\exp(-hc\nu_{b\leftarrow a}/k_BT)] \times R_v^2 F(m)L(J)\times 10^{-36}, \quad (13)$$

where I_x is the isotopic abundance of the corresponding isotopomer in the sample, $\nu_{b\leftarrow a}$ is the wavenumber of the transition (cm^{-1}), g_a is the nuclear-spin degeneracy factor, E_a is the energy of lower state (cm^{-1}), R_v^2 is the square of the rotationless transition dipole moment (Debye^2), $F(m) = (1 + A_1 m)^2$ is Herman–Wallis factor, and $m = -J$, $J + 1$ are for P and R branches, respectively; $L(J)$ is the Honl–London factor, and for $\Sigma - \Sigma$ transition, $L(J) = J$ and $J + 1$ are for P and R branches, respectively, $Q(T)$ is the total internal partition sum of molecules. Here, values of I_x, $\nu_{b\leftarrow a}$ and the ground vibrational state rotational energies E_a are taken from HITRAN database. The nuclear-spin degeneracy factor g_a for HO_2 is equal to 1. Using the line intensities of 010-000 transition of HO_2 in HITRAN database, we obtained the value of R_v^2 at 296 K. Then we further calculated the line intensities of 010-000 transition of HO_2 at 500 K and several higher temperatures.

3. Results and discussion

In Table 1, we compare the calculate the line intensities with available values from HITRAIN database for the ν_2 band of HO_2 at temperatures 500 and 3000 K. It can be seen that our values of line intensities are in very good agreement with those of HITRAN database at the temperatures up to 3000 K. The percent error among our calculated line intensities and those derived from HITRAN database is less than 0.511% and 0.659% at 500 and 3000 K, respectively. Such excellent agreements lend us much credibility in the calculations of partition function and line intensity at high temperatures. Thereby, we further calculate the line intensities at temperatures up to 4000 and 5000 K. The comparisons of our calculated simulated spectra of the 010-000 transition band of HO_2 with those from HITRAN database at 500 and 3000 K are shown in Fig.1. The percent error between the calculated line intensities and those derived from HITRAN database at 500 and 3000 K is shown in Fig.2. The spectral simulations at 4000 and 5000 K are shown in Fig.3.

Table 1. The line intensities data in the 010-000 band at different temperatures for HO_2 (unit: cm/molecule).

	500K			3000 K		40000 K	5000 K	
wavenumber	[a]S_{HITRAN}	[b]S_{calc}	[c]%	[a]S_{HITRAN}	[b]S_{calc}	[c]%	[b]S_{calc}	[b]S_{calc}
1333.133122	1.175×10^{-21}	1.174×10^{-21}	−0.126	4.079×10^{-23}	4.066×10^{-23}	−0.321	1.321×10^{-23}	5.139×10^{-24}
1337.512665	1.091×10^{-21}	1.090×10^{-21}	−0.112	4.029×10^{-23}	4.017×10^{-23}	−0.288	1.309×10^{-23}	5.104×10^{-24}
1339.862035	1.227×10^{-21}	1.226×10^{-21}	−0.096	3.982×10^{-23}	3.971×10^{-23}	−0.279	1.286×10^{-23}	4.994×10^{-24}
1342.204509	1.370×10^{-21}	1.369×10^{-21}	−0.085	3.926×10^{-23}	3.917×10^{-23}	−0.234	1.260×10^{-23}	4.878×10^{-24}
1344.540073	1.517×10^{-21}	1.522×10^{-21}	0.343	3.860×10^{-23}	3.868×10^{-23}	0.195	1.237×10^{-23}	4.771×10^{-24}
1346.283813	1.867×10^{-24}	1.866×10^{-24}	−0.055	4.245×10^{-26}	4.236×10^{-26}	−0.203	1.348×10^{-26}	5.180×10^{-27}
1348.594265	2.233×10^{-24}	2.228×10^{-24}	−0.215	4.556×10^{-26}	4.539×10^{-26}	−0.372	1.436×10^{-26}	5.502×10^{-27}
1350.047774	1.195×10^{-21}	1.193×10^{-21}	−0.165	3.420×10^{-23}	3.409×10^{-23}	−0.323	1.097×10^{-23}	4.246×10^{-24}
1352.108171	3.791×10^{-22}	3.787×10^{-22}	−0.094	3.215×10^{-23}	3.205×10^{-23}	−0.301	1.089×10^{-23}	4.355×10^{-24}
1355.60228	2.330×10^{-24}	2.327×10^{-24}	−0.111	4.895×10^{-26}	4.882×10^{-26}	−0.259	1.547×10^{-26}	5.934×10^{-27}
1357.061027	4.414×10^{-22}	4.415×10^{-22}	0.013	2.958×10^{-23}	2.953×10^{-23}	−0.165	9.918×10^{-24}	3.939×10^{-24}
1359.019755	6.007×10^{-24}	6.001×10^{-24}	−0.096	6.639×10^{-26}	6.624×10^{-26}	−0.227	2.033×10^{-26}	7.649×10^{-27}
1362.242551	6.042×10^{-24}	6.037×10^{-24}	−0.090	7.176×10^{-26}	7.159×10^{-26}	−0.230	2.206×10^{-26}	8.316×10^{-27}
1364.006982	5.549×10^{-22}	5.554×10^{-22}	0.090	2.692×10^{-23}	2.690×10^{-23}	−0.075	8.891×10^{-24}	3.497×10^{-24}
1366.726256	8.147×10^{-24}	8.140×10^{-24}	−0.092	8.421×10^{-26}	8.402×10^{-26}	−0.231	2.571×10^{-26}	9.653×10^{-27}
1368.004095	1.141×10^{-23}	1.140×10^{-23}	−0.091	9.604×10^{-26}	9.578×10^{-26}	−0.267	2.901×10^{-26}	1.083×10^{-26}
1372.009342	2.407×10^{-21}	2.408×10^{-21}	0.050	2.208×10^{-23}	2.206×10^{-23}	−0.084	6.711×10^{-24}	2.511×10^{-24}
1375.159769	1.952×10^{-24}	1.951×10^{-24}	−0.053	5.331×10^{-26}	5.320×10^{-26}	−0.204	1.709×10^{-26}	6.609×10^{-27}

Table 1 *Continued*

	500 K			3000 K			40000 K	5000 K
wavenumber	[a]S_{HITRAN}	[b]S_{calc}	[c]%	[a]S_{HITRAN}	[b]S_{calc}	[c]%	[b]S_{calc}	[b]S_{calc}
1380.068385	6.255×10^{-22}	6.254×10^{-22}	−0.019	1.712×10^{-23}	1.709×10^{-23}	−0.164	5.492×10^{-24}	2.124×10^{-24}
1385.140716	4.757×10^{-23}	4.740×10^{-23}	−0.365	2.965×10^{-25}	2.951×10^{-25}	−0.466	8.808×10^{-26}	3.259×10^{-26}
1387.92471	4.520×10^{-22}	4.518×10^{-22}	−0.034	4.146×10^{-24}	4.140×10^{-24}	−0.155	1.260×10^{-24}	4.715×10^{-25}
1389.995227	1.132×10^{-24}	1.129×10^{-24}	−0.285	7.946×10^{-27}	7.916×10^{-27}	−0.376	2.377×10^{-27}	8.827×10^{-28}
1391.950737	1.437×10^{-22}	1.437×10^{-22}	−0.001	8.993×10^{-25}	8.983×10^{-25}	−0.107	2.682×10^{-25}	9.926×10^{-26}
1393.038171	1.063×10^{-22}	1.062×10^{-22}	−0.119	1.278×10^{-24}	1.275×10^{-24}	−0.247	3.933×10^{-25}	1.484×10^{-25}
1393.977365	1.774×10^{-23}	1.772×10^{-23}	−0.122	5.871×10^{-25}	5.855×10^{-25}	−0.269	1.900×10^{-25}	7.392×10^{-26}
1395.056726	3.859×10^{-24}	3.855×10^{-24}	−0.092	3.239×10^{-26}	3.232×10^{-26}	−0.204	9.795×10^{-27}	3.657×10^{-27}
1397.007617	4.500×10^{-22}	4.497×10^{-22}	−0.078	4.587×10^{-24}	4.577×10^{-24}	−0.220	1.400×10^{-24}	5.260×10^{-25}
1399.05387	2.300×10^{-23}	2.300×10^{-23}	−0.009	2.589×10^{-25}	2.585×10^{-25}	−0.147	7.950×10^{-26}	2.995×10^{-26}
1400.532255	3.600×10^{-22}	3.600×10^{-22}	0.009	6.136×10^{-24}	6.127×10^{-24}	−0.143	1.924×10^{-24}	7.338×10^{-25}
1402.938896	2.005×10^{-21}	2.006×10^{-21}	0.037	1.284×10^{-23}	1.283×10^{-23}	−0.056	3.837×10^{-24}	1.421×10^{-24}
1404.337951	6.350×10^{-23}	6.333×10^{-23}	−0.273	3.855×10^{-24}	3.838×10^{-24}	−0.445	1.284×10^{-24}	5.089×10^{-25}
1406.002369	3.320×10^{-22}	3.319×10^{-22}	−0.019	8.167×10^{-24}	8.152×10^{-24}	−0.184	2.607×10^{-24}	1.006×10^{-24}
1408.551233	5.670×10^{-24}	5.665×10^{-24}	−0.090	1.610×10^{-25}	1.606×10^{-25}	−0.247	5.174×10^{-26}	2.004×10^{-26}
1410.160958	2.107×10^{-23}	2.104×10^{-23}	−0.152	1.492×10^{-25}	1.487×10^{-25}	−0.305	4.471×10^{-26}	1.661×10^{-26}
1412.137496	1.399×10^{-21}	1.395×10^{-21}	−0.259	1.375×10^{-23}	1.370×10^{-23}	−0.374	4.186×10^{-24}	1.571×10^{-24}
1414.925849	8.661×10^{-24}	8.673×10^{-24}	0.142	8.525×10^{-26}	8.525×10^{-26}	0.002	2.605×10^{-26}	9.777×10^{-27}
1417.155084	3.319×10^{-21}	3.317×10^{-21}	−0.049	2.738×10^{-23}	2.734×10^{-23}	−0.162	8.281×10^{-24}	3.091×10^{-24}
1419.264809	3.430×10^{-21}	3.428×10^{-21}	−0.062	3.139×10^{-23}	3.133×10^{-23}	−0.188	9.541×10^{-24}	3.573×10^{-24}
1421.258434	3.410×10^{-21}	3.409×10^{-21}	−0.037	3.339×10^{-23}	3.333×10^{-23}	−0.166	1.019×10^{-23}	3.822×10^{-24}
1423.336594	4.728×10^{-22}	4.720×10^{-22}	−0.161	1.005×10^{-23}	1.002×10^{-23}	−0.310	3.183×10^{-24}	1.222×10^{-24}
1427.934712	2.538×10^{-21}	2.537×10^{-21}	−0.021	3.358×10^{-23}	3.352×10^{-23}	−0.182	1.040×10^{-23}	3.938×10^{-24}
1429.322771	4.256×10^{-24}	4.250×10^{-24}	−0.147	5.748×10^{-26}	5.731×10^{-26}	−0.289	1.780×10^{-26}	6.746×10^{-27}
1431.075816	2.686×10^{-21}	2.686×10^{-21}	−0.009	3.982×10^{-23}	3.977×10^{-23}	−0.131	1.241×10^{-23}	4.716×10^{-24}
1433.16859	2.769×10^{-21}	2.763×10^{-21}	−0.219	4.379×10^{-23}	4.362×10^{-23}	−0.390	1.366×10^{-23}	5.200×10^{-24}
1435.129003	2.449×10^{-21}	2.446×10^{-21}	−0.110	4.299×10^{-23}	4.288×10^{-23}	−0.254	1.350×10^{-23}	5.155×10^{-24}
1437.176485	2.025×10^{-24}	2.021×10^{-24}	−0.181	4.648×10^{-26}	4.633×10^{-26}	−0.330	1.478×10^{-26}	5.691×10^{-27}
1439.063997	2.086×10^{-21}	2.089×10^{-21}	0.140	4.367×10^{-23}	4.365×10^{-23}	−0.040	1.386×10^{-23}	5.323×10^{-24}
1440.149139	1.787×10^{-21}	1.781×10^{-21}	−0.356	4.238×10^{-23}	4.218×10^{-23}	−0.481	1.348×10^{-23}	5.195×10^{-24}
1442.736357	1.552×10^{-24}	1.544×10^{-24}	−0.511	4.128×10^{-26}	4.101×10^{-26}	−0.659	1.318×10^{-26}	5.098×10^{-27}
1446.708035	1.169×10^{-21}	1.169×10^{-21}	−0.010	4.405×10^{-23}	4.395×10^{-23}	−0.228	1.437×10^{-23}	5.619×10^{-24}
1450.793932	7.544×10^{-22}	7.524×10^{-22}	−0.263	3.935×10^{-23}	3.917×10^{-23}	−0.455	1.302×10^{-23}	5.141×10^{-24}
1455.705068	4.761×10^{-22}	4.762×10^{-22}	0.021	3.734×10^{-23}	3.728×10^{-23}	−0.170	1.265×10^{-23}	5.056×10^{-24}
1457.777878	4.105×10^{-22}	4.107×10^{-22}	0.057	3.671×10^{-23}	3.665×10^{-23}	−0.152	1.252×10^{-23}	5.024×10^{-24}
1459.71754	3.673×10^{-22}	3.670×10^{-22}	−0.070	3.742×10^{-23}	3.731×10^{-23}	−0.297	1.283×10^{-23}	5.168×10^{-24}
1459.717544	3.673×10^{-22}	3.670×10^{-22}	−0.070	3.742×10^{-23}	3.731×10^{-23}	−0.297	1.283×10^{-23}	5.168×10^{-24}

Notes: [a]values from HITRAIN database; [b]values from the calculated in this work; [c]percent error between S_{HITRAN} and S_{calc}.

In line intensity calculation formula (13), the square of rotationless transition dipole moment R_{v}^2 can be expressed as

$$R_{\mathrm{v}}^2 = \left| \int \psi_{\mathrm{v}}' \boldsymbol{d} \psi_{\mathrm{v}}'' \mathrm{d}\tau \right|^2 . \tag{14}$$

In Eq.(14), the wavefunctions ψ_{v}', ψ_{v}'' and electronic dipole moment $\boldsymbol{d}$ are functions of the nuclear displacement coordinates. That is to say, the square of rotationless transition dipole moment R_{v}^2 is dependent on the molecular structure. The theoretical calculation on equation of state for detonation products (CO_2, O_2 and H_2O etc.) of CHNO explosives shows that the molecular structure of CO_2, O_2 and H_2O etc. almost do not change at temperatures up to 5000 K. Therefore, R_{v}^2 can be regarded as a constant.

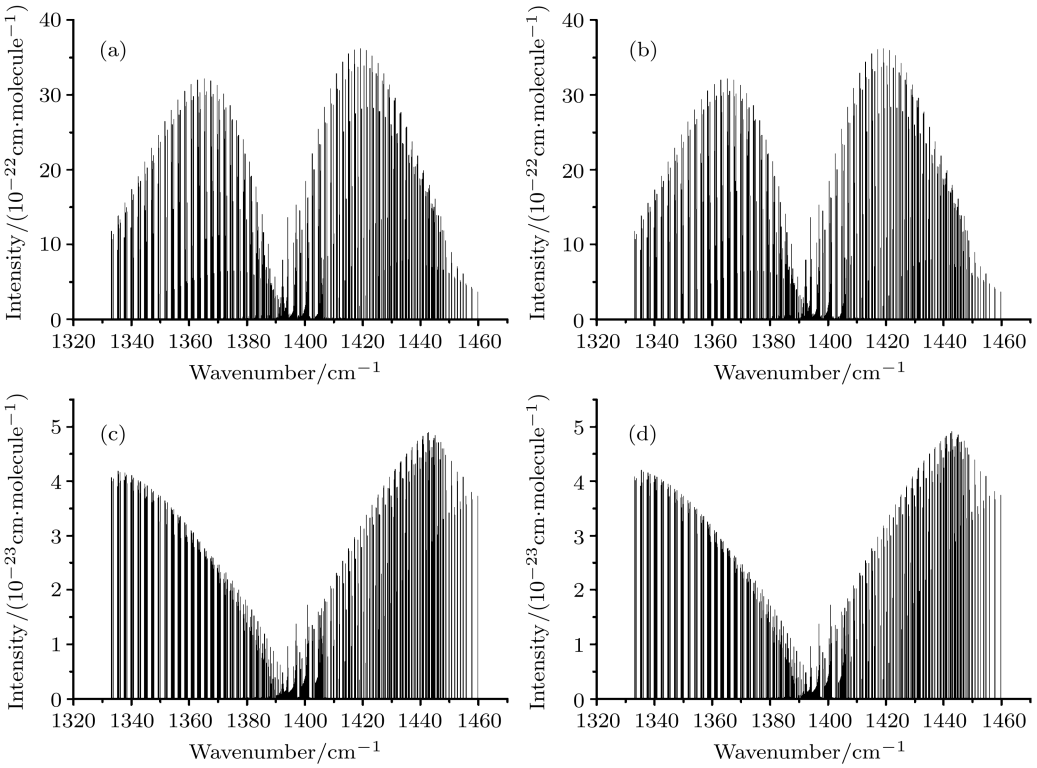


Fig.1. Comparison of our line intensities data in the 010-000 band with the data in HITRAN database for HO_2 (a) 500 K, calculated in this work; (b) 500 K, from HITRAN; (c) 3000 K, calculated in this work; (d) 3000 K, from HITRAN.

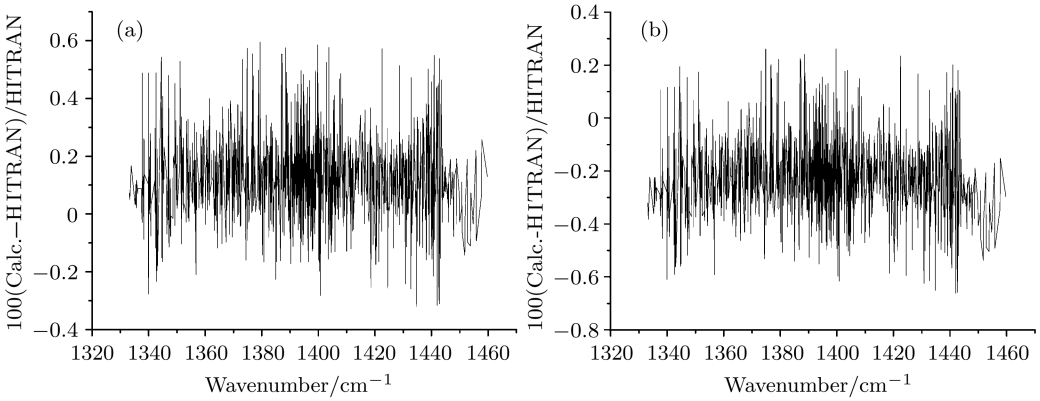


Fig.2. Percent error between the calculated line intensities and the data in HITRAN database for (a) 500 K; (b) 3000 K.

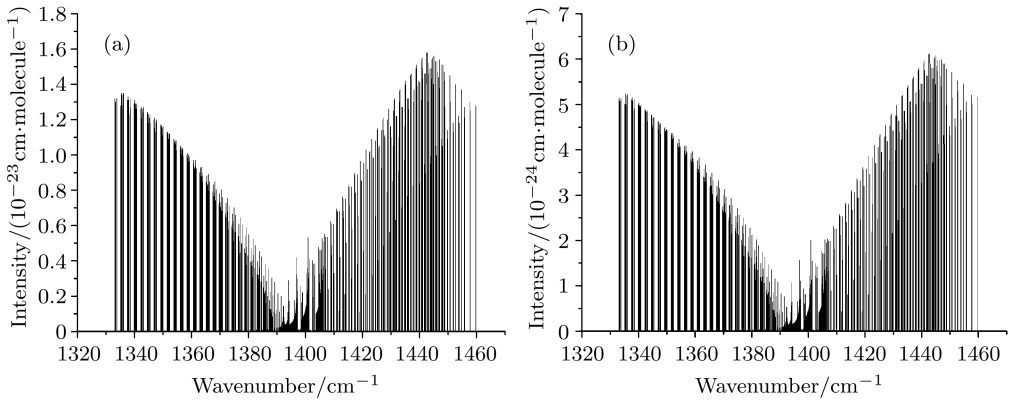


Fig.3. The simulated spectra of 010-000 band of HO_2 at (a) 4000 K; (b) 5000 K.

Besides R_v^2, Herman–Wallis factor $F(m)$ and the Honl–London factor $L(J)$ are independent of temperature T in Eq.(13), and only the partition function $Q(T)$ depends on T. Therefore, as long as the partition function $Q(T)$ is calculated with sufficient accuracy, the line intensities at high temperatures should be credible with the same accuracy. Of course, as a result of product approximation, TIPS at high temperatures would have a certain error, which in turn will produce an error of line intensities at high temperatures. The value of error should be verified by experiments.

4. Conclusion

The total internal partition functions have been calculated for temperatures up to 5000 K for the asymptotic asymmetric-top molecule HO_2 in the product approximation. The rotational partition functions were obtained with the analytical expression of Watson and the vibrational partition functions with the harmonic oscillator approximation. Using the calculated partition functions and the rotationless transition dipole moment squared and Herman–Wallis factor, we have computed the line intensities of ν_2 band of the asymptotic asymmetric-top HO_2 molecule at temperatures 500, 3000, 4000, and 5000 K. The line intensities and simulated spectra are in very good agreement with those in HITRAN database for temperatures 500 and 3000 K. We believe that the simulated spectra of ν_2 band of HO_2 radical at temperatures 4000 and 5000 K should be reliable. This is of importance for retrieval of information of the asymptotic asymmetric-top molecule spectra at high temperatures.

References

[1] Herzberg G 1947 *Molecular Spectra and Molecular Structure* I. *Spectra of Diatomic Molecules* (New York: D.Van Nostrand) p1

[2] Hong G L, Zhang Y C, Zhou M R, Cao K F and Zhou J 2006 *Spectroscopy and Spectral Analysis* **26** 1249 (in Chinese)

[3] Wan F X, Zhang Z Y and Wang Y M 2006 *Spectroscopy and Spectral Analysis* **26** 908 (in Chinese)

[4] Jacox M E and Milligan D E 1972 *J. Mol. Spectrosc.* **42** 495

[5] Hougen J T, Radford H E, Evenson K M and Howard C J 1975 *J. Mol. Spectrosc.* **56** 210

[6] Lightfoot P D and Jemi-Alade A A 1991 *J. Photochem. Photobiol.* A: *Chem.* **59** 1

[7] Barnes C E, Brown J M and Radford H E 1980 *J. Mol. Spectrosc.* **84** 179

[8] Mcadam K, Veyret B and Lesclaux R 1987 *Chem. Phys. Lett.* **133** 39

[9] Liu A W, Hu S M, Ding Y and Zhu Q S 2005 *Chin. Phys.* **14** 1946

[10] Xu C Y, Yang X H, Guo Y C, Wu L, Li W and Chen Y Q 2005 *Chin. Phys.* **14** 1954

[11] Chen P, Zhu H, Hao L Y, Hu S M, Liu A W, Zheng J J and Ding Y 2005 *Chin. Phys.* **14** 634

[12] Han H X, Peng Q, Wen Z Y and Wang Y B 2005 *Acta Phys. Sin.* **54** 78 (in Chinese)

[13] Ma S H, Shi Y L, Xu X L, Yan W, Yang Y P and Wang L 2006 *Acta Phys. Sin.* **55** 4091 (in Chinese)

[14] Zhang Q L, Wang L, Weng Y X, Qiu X G, Wang W C and Yan J X 2005 *Chin. Phys.* **14** 2484

[15] Gou Q Q and Zhu J 2001 *Chin. Phys.* **10** 286

[16] Wang W N, Li Y B and Yue W W 2007 *Acta Phys. Sin.* **56** 781 (in Chinese)

[17] Rothman L S, Jacquemart D, Barbe A, Benner D C, Birk M, Brown L R, Carleer M R, Chackerian-Jr C, Chance K, Coudert L H, Dana V, Devi V M, Flaud J M, Gamache R R, Goldman A, Hartmann J M, Jucks K W, Maki A G, Mandin J Y, Massie S T, Orphal J, Perrin A, Rinsland C P, Smith M A H, Tennyson J, Tolchenov R N, Toth R A, Auwera J V, Varanasi P and Wagner G 2005 *J. Quant. Spectrosc. Radiat. Transfer* **96** 139

[18] Song X S, Cheng X L, Yang X D and Linghu R F 2007 *Acta Phys. Sin.* **56** 4428 (in Chinese)

[19] Song X S, Yang X D, Guo Y D, Wang J, Cheng X L and Linghu R F 2007 *Communications in Theoretical Physics* **47** 892

[20] Song X S and Yang X D 2007 *Chin J. At. Mol. Phys.* **24** 435 (in Chinese)

[21] Gamache R R, Kennedy S, Hawkins R L and Rothman L S 2000 *J. Mol. Struct.* **517–518** 407

[22] Herzberg G 1947 *Molecular Spectra and Molecular Structure* II. *Infrared and Raman Spectra of Polyatomic Molecules* (New York: Van Nostrand) p76

[23] Watson J K G 1988 *Mol. Phys.* **65** 1377

[24] Barnes C E, Brown J M, Carrington A, Pinkstone J, Sears T J and Thistlethwait P J 1978 *J. Mol. Spectrosc.* **72** 86

[25] Norton R H and Rinsland C P 1991 *Appl. Opt.* **30** 389

[26] Claveau C, Teffo J L, Hurtmans D, Valentin A and Gamache R R 1999 *J. Mol. Spectrosc.* **193** 15